Supplemental material

Ferrovalley and topological phase transition behaviors in monolayer $Ru(OH)_2$

Yanzhao Wu[a], Li Deng[a], Junwei Tong[b], Xiang Yin[a], Fubo Tian[c], Gaowu Qin[a] and Xianmin Zhang[a]*
[a]Key Laboratory for Anisotropy and Texture of Materials (Ministry of Education), School of Material Science and Engineering, Northeastern University, Shenyang, 110819, China
[b]Department of Physics, Freie Universität Berlin, Berlin, 14195, Germany
[c]State Key Laboratory of Superhard Materials, College of Physics, Jilin University, Changchun, 130012, China

*E-mail: zhangxm@atm.neu.edu.cn

Figure S1 displays one ferromagnetic (FM) and one antiferromagnetic (AFM) configurations of monolayer $Ru(OH)_2$.

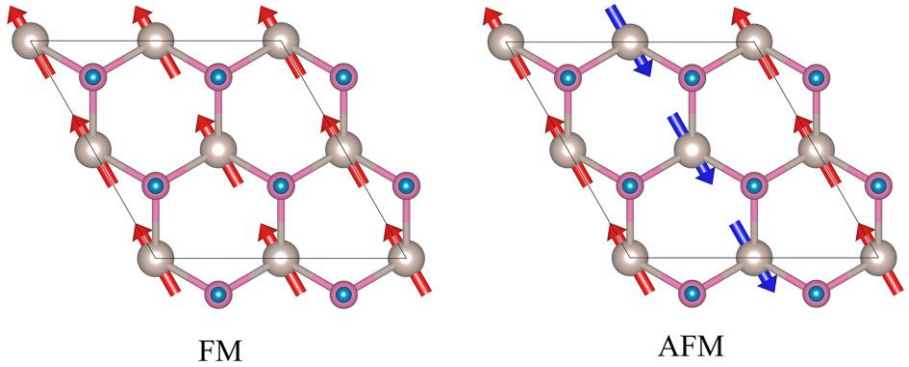

Figure S1. One ferromagnetic (FM) and one antiferromagnetic (AFM) configurations of monolayer $Ru(OH)_2$.

Figure S2 shows the spin charge density distribution of monolayer $Ru(OH)_2$ under FM and AFM states, respectively. It can be seen that the spin charge density of both spin-up (yellow in Figure S2) and spin-down (cyan in Figure S2) orientations is mainly concentrated on the Ru atoms, while the spin charge density of O and H atoms is absent. This proves that the magnetic moment of monolayer $Ru(OH)_2$ is mainly contributed by the Ru atoms.

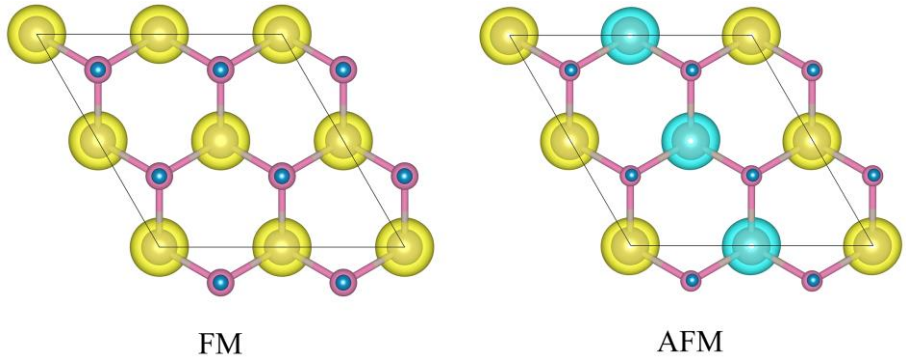

Figure S2. Spin charge density of monolayer Ru(OH) under FM and AFM states. The yellow and cyan represent spin-up and spin-down charge densities, respectively. The isovalue is 0.037 e/Bohr^3.

Figure S3(a) shows the spin-resolved band structure of monolayer $Ru(OH)_2$ without ferromagnetism under the SOC effect. It is found that the fermi level crosses the energy band, which results in a metal characteristic for present monolayer $Ru(OH)_2$. Moreover, the degeneracy of K and K′ valleys for the same spin (red and blue) is still broken owing to the lack of space inversion symmetry [1, 2]. However, when the up and down spins are considered simultaneously, K and K′ valleys are energetically degenerate due to the time reversal symmetry of the monolayer $Ru(OH)_2$ [3, 4]. Figures S3(b) – S3(f) show the d-orbitals projected band structures of Ru atoms in the $Ru(OH)_2$ monolayer. The valley states at the K and K′ points are mainly contributed by the occupied d_{xy} and $d_{x^2-y^2}$ orbitals of Ru atom, as shown in Figures S3 (b) and S3(c). The d_{z^2} orbitals of Ru atoms are mainly distributed near the K and K′ points of the conduction band, as displayed in Figure S3(d). Comparatively, the electronic states of d_{xz} and d_{yz} orbitals of the Ru atoms far away from the Fermi level, so it has little contribution to the valley electron state, as shown in Figures S3(e) and S3(f).

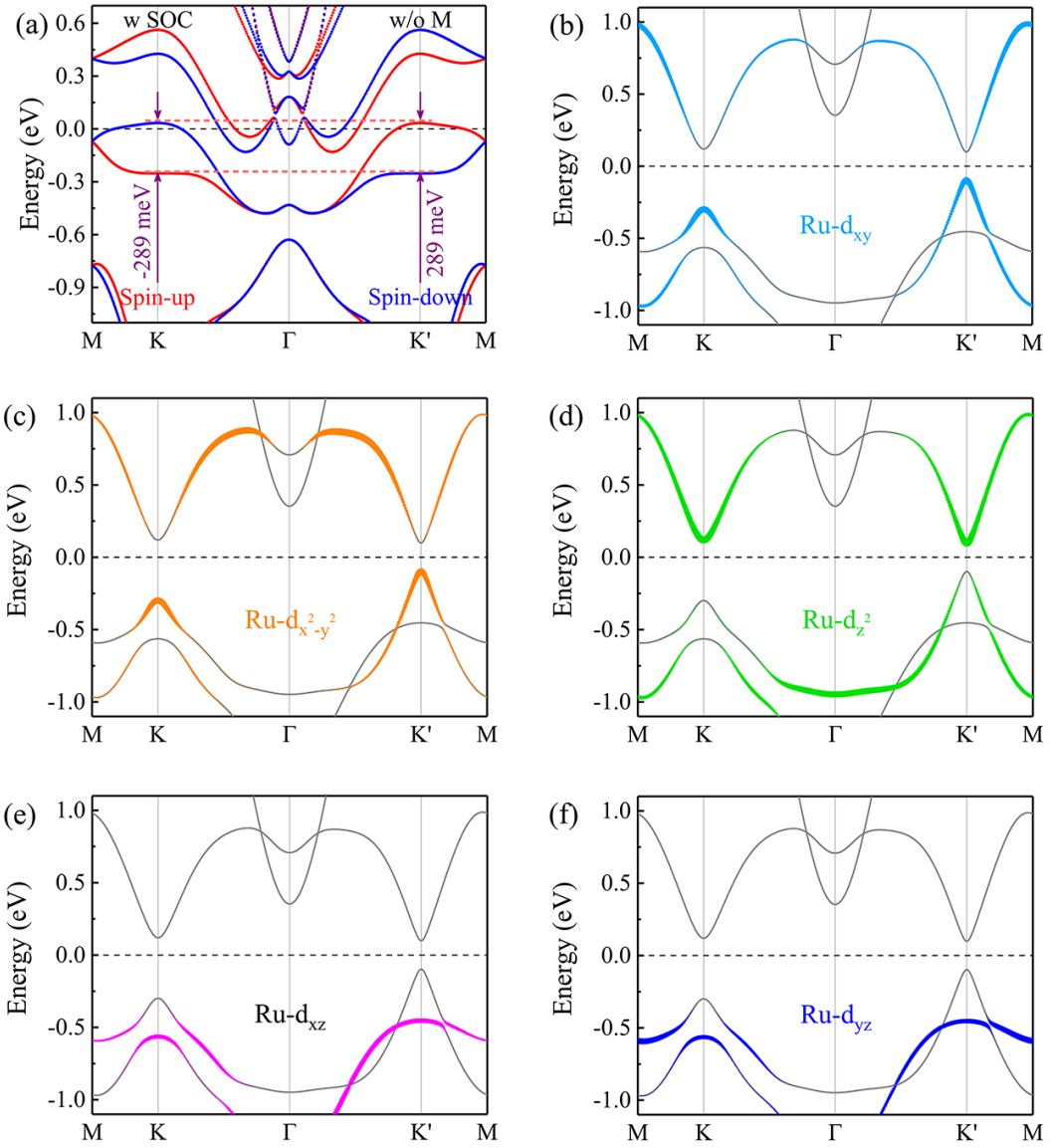

Figure S3. (a) Spin-resolved band structure of monolayer $Ru(OH)_2$ without ferromagnetism under the SOC effect. (b)-(f) Projected band structures of Ru-d orbitals for monolayer $Ru(OH)_2$.

Figure S4 shows the T_C and T_{BKT} of monolayer $Ru(OH)_2$ with different biaxial strains. As shown in Figure S4(a), under 0% ~ -3% strains, the T_C of monolayer $Ru(OH)_2$ increases with the increasing of compressive strain. The T_C of monolayer $Ru(OH)_2$ reaches 623 K at -3% compressive strain. Comparatively, with 0% ~ 3% strains, the T_C of monolayer $Ru(OH)_2$ decreases with the enlarging of tensile strain. At 3% strain, the T_C of monolayer $Ru(OH)_2$ becomes 64 K. Comparatively, as the strain changes from -3% to 3%, the T_{BKT} of monolayer $Ru(OH)_2$ decreases from 742 to 76 K, as shown in Figure S4(b).

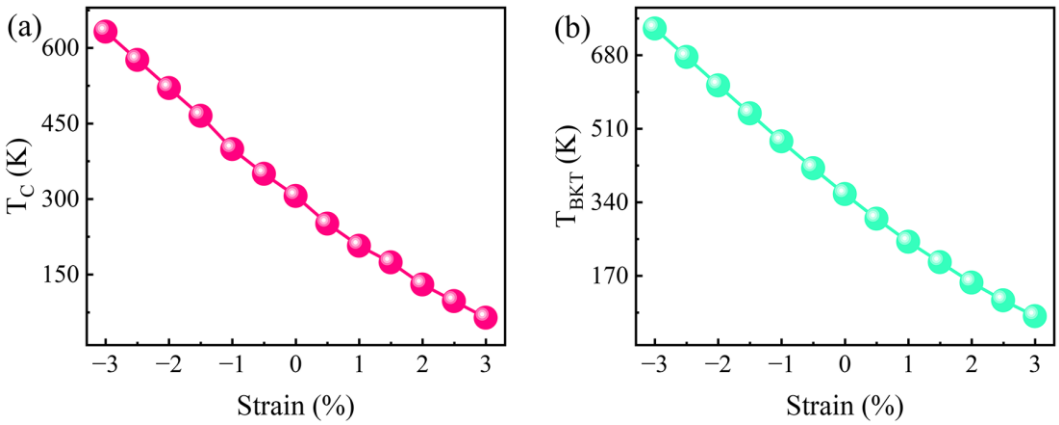

Figure S4. The T_C and T_{BKT} of monolayer $Ru(OH)_2$ with different biaxial strains.

Figure S5 shows the SOC band structures of monolayer Ru $(OH)_2$ at -1, -2 and -3% compressive strains, respectively. It could be seen that monolayer Ru $(OH)_2$ is always a FV semiconductor during the whole compressive strain progress. Moreover, the valley polarizations are -198 meV, -196 meV and -193 meV for monolayer Ru $(OH)_2$ at -1, -2 and -3% compressive strains, respectively.

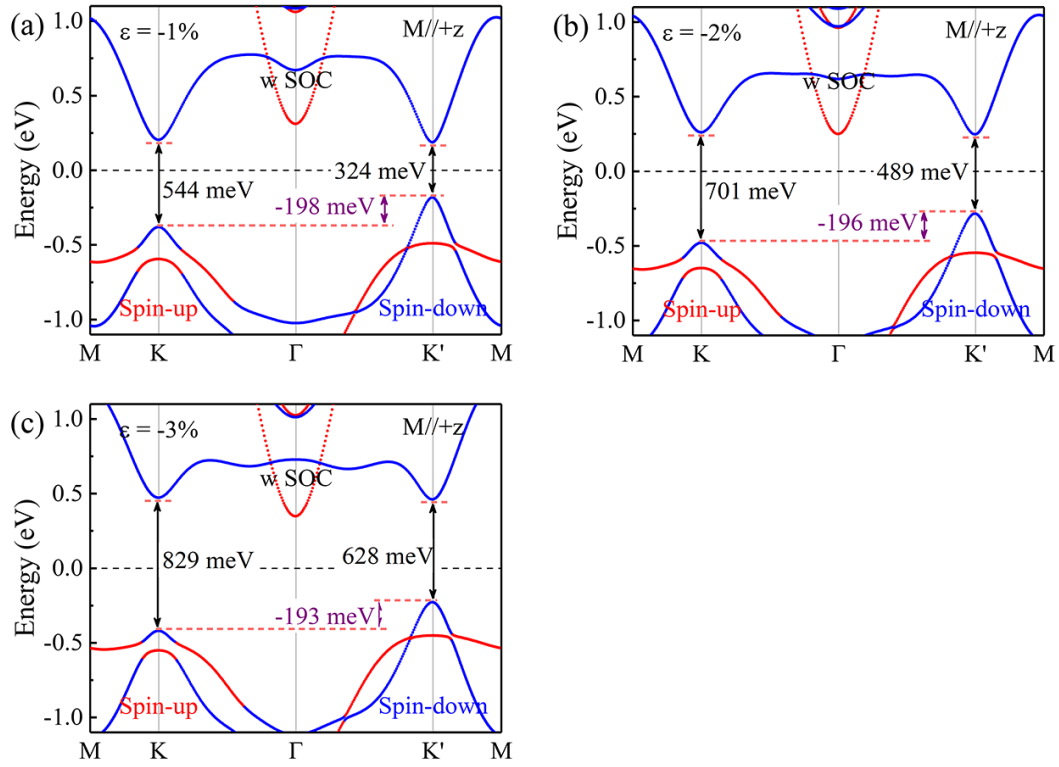

Figure S5. Spin-resolved band structures of monolayer Ru $(OH)_2$ at (a) -1, (b) -2 and (c) -3% compressive strains under the SOC effect, respectively.

As observed in Figure S6(a), the Fermi energy level crosses the K′ valley of the spin-down channel in monolayer $Ru(OH)_2$ with doping 0.05 holes/f.u., which means carriers with 100% spin-down state are dominated by the K′ valley. This is a typical characteristic of half metal. As the magnetization of the Ru atom reversing to the -z direction, carriers with 100% spin-up state are dominated by the K valley, as shown in figure S6(b). Such special half-metallic materials with a metallic character in one spin channel and a semiconducting nature in the other could provide completely spin-polarized current for highly efficient spintronics devices [5, 6]. The calculated Berry curvature further indicates valley contrasting characteristic, as indicated in Figure S6(c). As shown in Figure S6(d), the Fermi level lies between the K and K′ valleys, as denoted with two vertical dashed lines (green region), which also means a fully spin- and valley-polarized Hall conductivity is generated [7]. In the first-principles calculations, carrier doping is simulated by removing or adding electrons from the system and using a homogeneous background charge to maintain charge neutrality [5, 6].

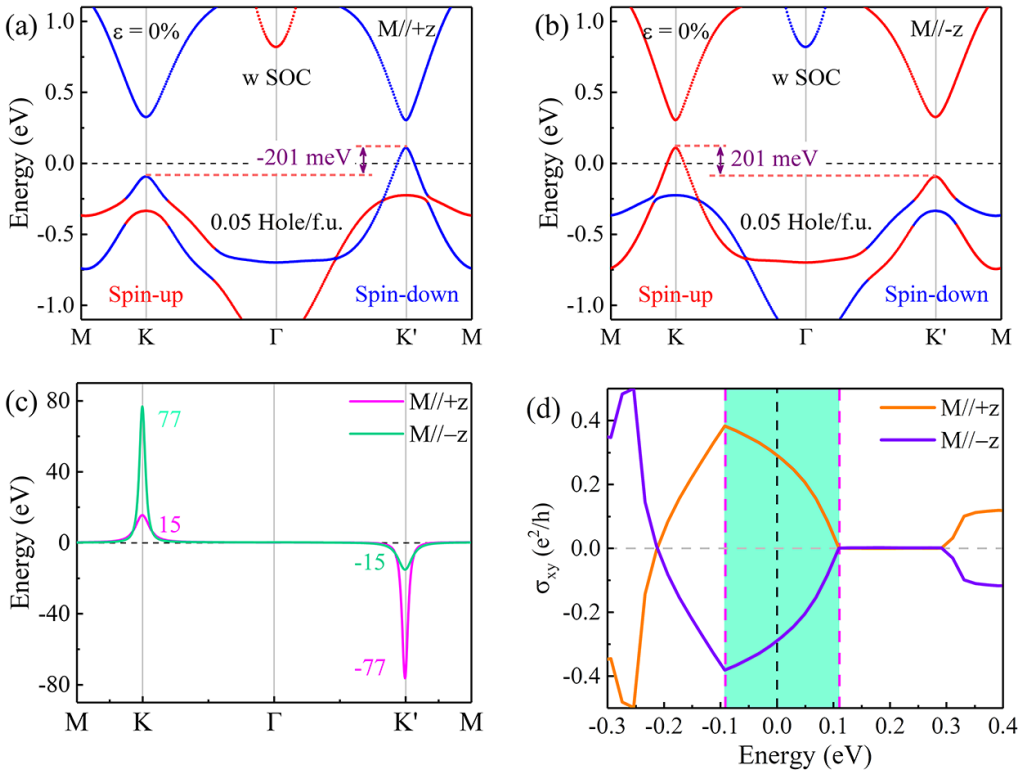

Figure S6. Spin-resolved band structures under the SOC effect of monolayer Ru $(OH)_2$ with doping 0.05 holes/f.u.. for the magnetization of the Ru atom along the (a) +z and (b) -z directions, respectively. (c) Berry curvature along the high symmetry line for monolayer $Ru(OH)_2$ with doping 0.05 holes/f.u.. (d) Anomalous Hall conductivity σ_{xy} as a function of Fermi energy for monolayer $Ru(OH)_2$ with doping 0.05 holes/f.u.. The two vertical dashed lines (green region) denote the two valley extrema.

As observed in Figure S7(a), with doping 0.05 electrons/f.u., the Fermi energy level crosses the K valley of the spin-down channel in monolayer $Ru(OH)_2$ under 3% tensile strain. Therefore, carriers with 100% spin-down state are dominated by the K valley. As the magnetization of the Ru atom reversing to the -z direction, carriers with 100% spin-up state are dominated by the K′ valley, as shown in figure S7(b). The calculated Berry curvature further indicates valley contrasting characteristic, as indicated in Figure S7(c). As drawn in Figure S7(d), the Fermi level lies between the K and K′ valleys, as denoted with two vertical dashed lines (green region), which also means a fully spin- and valley-polarized Hall conductivity is generated.

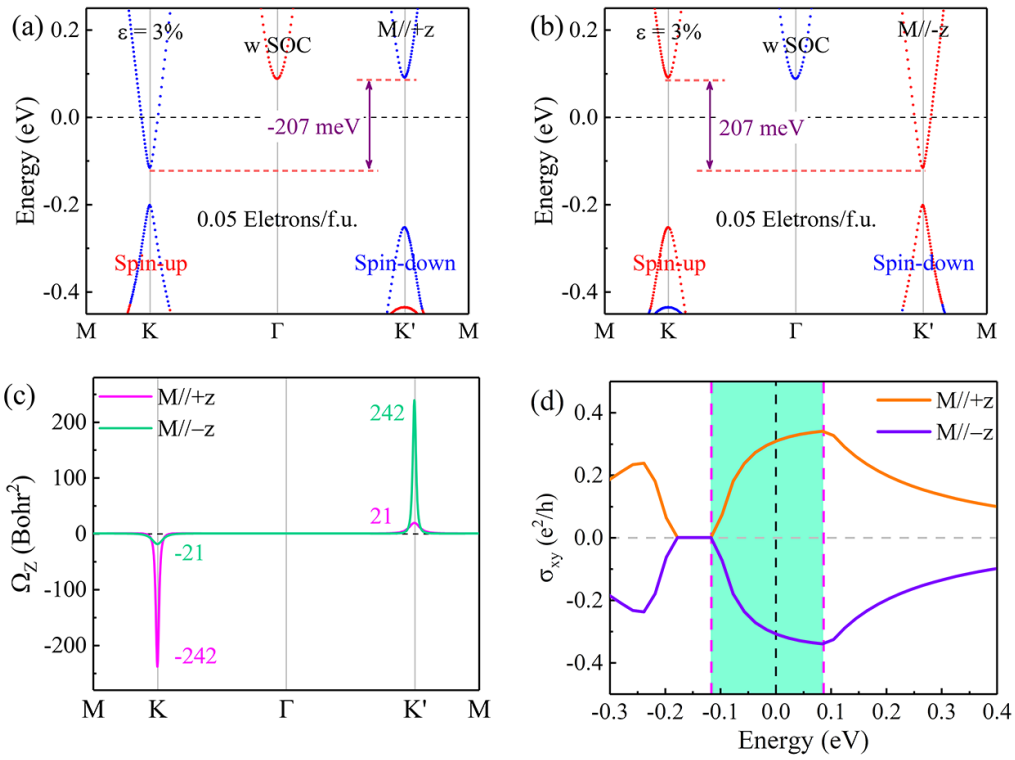

Figure S7. Spin-resolved band structures with SOC effect of monolayer Ru $(OH)_2$ under 3% tensile strain with doping 0.05 electrons/f.u.. for the magnetization of the Ru atom along the (a) +z and (b) -z directions, respectively. (c) Berry curvature along the high symmetry line for monolayer $Ru(OH)_2$ with doping 0.05 electrons/f.u.. (d) Calculated anomalous Hall conductivity σ_{xy} as a function of Fermi energy for monolayer $Ru(OH)_2$ with doping 0.05 electrons/f.u.. The two vertical dashed lines (green region) denote the two valley extrema.

At the last, the crystal structure of monolayer $Ru(OH)_2$ is listed so that our calculated results can be replicated by others, as shown in Figure S8.

```
Ru(OH)2
   1.00000000000000
     3.2845963898137049     0.0000000000000000     0.0000000000000000
    -1.6422981949068525     2.8445439147573222     0.0000000000000000
     0.0000000000000000     0.0000000000000000    21.4142858976110801
     Ru      O      H
     1       2      2
Direct
  0.0000000000000000  0.0000000000000000  0.5000000000000000
  0.3333333333333357  0.6666666666666643  0.5609159405585774
  0.3333333333333357  0.6666666666666643  0.4390840594414225
  0.3333333333333357  0.6666666666666643  0.6062190847128863
  0.3333333333333357  0.6666666666666643  0.3937809152871137
```

Figure S8. The crystal structure of monolayer $Ru(OH)_2$.

References

[1] W.-Y. Tong, S.-J. Gong, X. Wan, and C.-G. Duan, Concepts of ferrovalley material and anomalous valley Hall effect, *Nature Communications* **7**, 13612 (2016).

[2] K. Sheng, Q. Chen, H.-K. Yuan, and Z.-Y. Wang, Monolayer CeI_2: an intrinsic room-temperature ferrovalley semiconductor, *Physicals Review B* **105**, 075304 (2022).

[3] S.-D. Guo, J.-X. Zhu, W.-Q. Mu, and B.-G. Liu, Possible way to achieve anomalous valley Hall effect by piezoelectric effect in a $GdCl_2$ monolayer, *Physicals Review B* **104**, 224428 (2021).

[4] Y. Wu, J.i Tong, L. Deng, F. Luo, F. Tian, G. Qin, and X. Zhang, Realizing spontaneous valley polarization and topological phase transitions in monolayer ScX_2 (X = Cl, Br, I), *Acta Materialia* **246**, 118731 (2023).

[5] X. Li, X. Wu, and J. Yang, Half-Metallicity in $MnPSe_3$ Exfoliated Nanosheet with Carrier Doping, *Journal of the American Chemical Society* **136**, 11065 (2014).

[6] Y. Chen, Q. Fan, Y. Liu, and G. Yao, Electrically tunable magnetism and unique intralayer charge transfer in Janus monolayer MnSSe for spintronics applications, *Physicals Review B* **105**, 195410 (2022).

[7] H.-X. Cheng, J. Zhou, W. Ji, Y.-N. Zhang, and Y.-P. Feng, Two-dimensional intrinsic ferrovalley GdI_2 with large valley polarization, *Physicals Review B* **103**, 125121 (2021).